11th World Congress on Computational Mechanics (WCCM XI)
5th European Conference on Computational Mechanics (ECCM V)
6th European Conference on Computational Fluid Dynamics (ECFD VI)
E. Oñate, J. Oliver and A. Huerta (Eds)

A NEW FEM HOMOGENIZATION OF PERIODIC MATERIAL BASED ON AN EXTENDED ROSETTE GAGE THEORY

LUIS PÉREZ POZO[†], MAREK KOLENDO [‡], SERGIO OLLER [*], SHEILA LASCANO [†] AND CLAUDIO AGUILAR [**]

[†] Department of Mechanical Engineering, Aula UTFSM-CIMNE
Universidad Técnica Federico Santa María, Chile

[‡] Department of Biomedical Engineering
Universität Stuttgart, Germany

[*] International Center for Numerical Methods in Engineering (CIMNE)
Universidad Politécnica de Cataluña, Spain

[**] Departament of Metalurgical and Materials Engineering
Universidad Técnica Federico Santa María, Chile

Key words: Finite Element, homogenization, Strain Transformation, Rosette Gage Theory

Abstract. A long-known research area is the theoretical consideration of strengths behavior for material consisting of a highly complex micro-structure due to irregular forms and shape distributions or a composition of different materials. The fundamental theory underlying these research work is the homogenization theory. Common analytical and micro-mechanical homogenization techniques are mathematically complex and mainly constructed only for special statements of the problem. Numerical approaches require the consideration of particular boundary conditions and the examination of a so called representative volume element (RVE). Present work aims at an alternative strategy where the evaluation of homogenized strength parameters can be obtained through simple strain and stress measuring in an extended strain rosette. Foundation hereby is the application of constitutive equations from the strain transformation and rosette gage theory on measured values obtained through a 2D static structural FEM simulation of a Representative Material Section (RMS) of the considered inhomogeneous material. The major advantage of the present technique is both, the reduction of computational time compared to the full model and compared to other homogenization methods, the low modeling effort. To verify the method it will be shown that the homogenized Young's modulus and homogenized Poisson's ratio of a carbon/epoxy composite structure obtained by the new homogenization method points out good match with a well established Finite Element Multiscale Homogenization method.

1 INTRODUCTION

Homogenization in mechanics is the description of a highly complex structured material through a special model which strongly facilitates this structure and is still able to simulate plausible behavior in deformation for the analyzed loading cases.
The basic idea of every homogenization method is to assume the macro model being homogeneous hence the geometry can be meshed with a coarser mesh. This leads consequently to a great reduction of the degree of freedom. The influence of the micro-structure on the replacement body depends on the chosen homogenization technique. The conclusion of all homogenization techniques can be categorized into Micro-Mechanics Homogenization, Numerical Homogenization and Mathematical Homogenization. In addition it is convenient to make a differentiation between periodic and non-periodic material structures. Present paper is focused on former material structure [1].
Micro-Mechanic Homogenization is topic of research and intensively investigated for more than 60 years now. There exist various theories and applications. The most basic concepts although are all relevant to the "Eshelby Problem". More precisely they use the Eshelby-Tensor to define Concentration-Tensors that allow in turn the formulation of elastic moduli. In consequence of using the Eshelby-Tensor, they solely consider the shape of the inhomogeneities but not their size and spatial distribution in the material. The Eshelby-Method builds directly upon the solutions of the Eshelby-Problem and is applied to composites where interactions and mutual impact of individual inhomogeneities can be neglected [2]. To overcome this issue, the Mori-Tanaka-Scheme was developed. Unlike the Eshelby-Method this method considers at the infinite remote contour of the medium not the initially applied loading, but the volumetric average strain of the matrix material. Thereby interactions and mutual impact of different inhomogeneities can be treated [3].
Numeric Homogenization considers directly the detailed modeled RVE. The microscopic material response can be simulated by means of the FEM or another numerical method. The corresponding macroscopic strengths behavior can be obtained by using volumetric averaging over the RVE. Due to the general approach of the Numerical Homogenization it can be applied to every material model as long the RVE is able to describe the geometrical and material heterogeneities. The main effort is therefore to specify an adequate RVE. In literature there exist several stochastic approaches to obtain the optimal size of the RVE. The work of Gitman [4] and Kanit [5] demonstrate well established solutions for this problem.
Present work demonstrates an alternative homogenization method where the determination of an adequate RVE can be neglected. Furthermore the interactions and mutual impact of individual inhomogeneities can be taken into account and composites with a volumetric high percentage of fibers can therefore be considered as well. The basic idea is to simulate the electrical metrology of a Rosette Gage in a FEM analysis to obtain a homogenized Poisson's ratio. In a subsequent analysis the strain gage rosette is extended to multiple gages where the average stress along the gages is evaluated and averaged.

With the homogenized Poisson's ratio of the proceeding measurement Hooke's Law can be applied to solve the Young's modulus for every gage direction. In conclusion, the homogenized Young's modulus is computed as the average of all considered gage directions.

2 FORMULATION

2.1 Strain Gage Rosette

A rosette strain gage is an electromechanical device that can measure relative surface elongations in three directions. Bonding such a device to the surface of a structure allows determination of elongational strains in particular directions. Due to the fact, that the 2D state of strain at a point (on a surfcace) is defined by three independent quantities which can be taken as either: (a) ϵ_x, ϵ_y, and γ_{xy} or (b) ϵ_1, ϵ_2 and ϕ, where case (a) refers to strain components with respect to an arbitrary xy axis system, and case (b) refers to the principal strains and their directions. Either case fully defines the state of 2D strain on the surface and can be used to compute strains with respect to any other coordinate system. To determine the three independent quantities it is necessary to place three strain gages together in a "rosette" (see Fig. 1-(a)) with each gage oriented in a different direction and with all of them located as close as possible together to approximate a measurement at a point. An overview about different gages and it's metrology can be found in ref. [6].

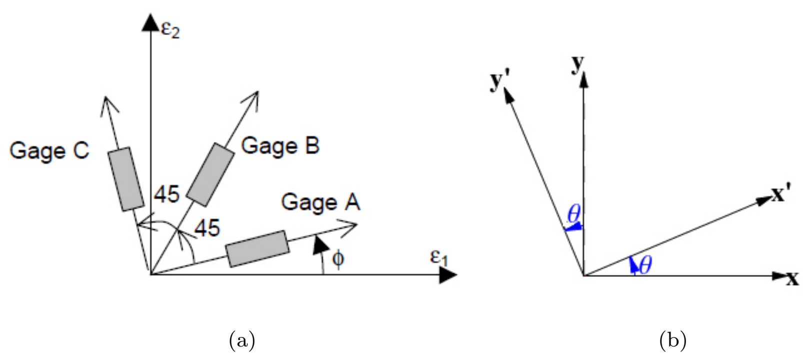

Figure 1: (a) Rectangle Rosette Gage Orientation and (b) Two-dimensional rotational transformation.

If the three strains and the gage directions are known, it is possible to solve for the principal strains and their directions or equivalently, the state of strain with respect to an arbitrary xy coordinate system. The relations needed can be obtained from the strain transformation theory. The strains are components of a symmetric second-order tensor (see for derivation ref. [7]) thus the general transformation properties between Cartesian coordinate systems can be applied to get the strain components described in one coordinate system for any other rotated system. To demonstrate the strain transformation relations the strain tensor $\boldsymbol{\varepsilon}$ first will be written in matrix format:

$$\boldsymbol{\varepsilon} = \left[\ \varepsilon\ \right] = \begin{bmatrix} \varepsilon_x & \varepsilon_{xy} & \varepsilon_{xz} \\ \varepsilon_{xy} & \varepsilon_y & \varepsilon_{yz} \\ \varepsilon_{xz} & \varepsilon_{yz} & \varepsilon_z \end{bmatrix}, \tag{1}$$

according to the coordinate system shown in Fig. 1-(b), the transformed elastic tensor can be written as:

$$\mathbf{e}^{'}_{ij} = \mathbf{Q}_{ip}\mathbf{Q}_{jq}\boldsymbol{\varepsilon}_{pq} \tag{2}$$

where the rotation matrix $\mathbf{Q}_{ij} = cos(x^{'}_i, x_j)$. For the two-dimensional case shown in Fig.2, the transformation matrix can be expressed as:

$$\mathbf{Q}_{ij} = \begin{bmatrix} cos\theta & sin\theta & 0 \\ -sin\theta & cos\theta & 0 \\ 0 & 0 & 1 \end{bmatrix}. \tag{3}$$

Under this transformation, the in-plane strain components transform according to:

$$\begin{aligned} \varepsilon^{'}_x &= \varepsilon_x cos^2\theta + \varepsilon_y sin^2\theta + 2\varepsilon_{xy} sin\theta cos\theta \\ \varepsilon^{'}_y &= \varepsilon_x sin^2\theta + \varepsilon_y cos^2\theta - 2\varepsilon_{xy} sin\theta cos\theta \\ \varepsilon^{'}_{xy} &= -\varepsilon_x sin\theta cos\theta + \varepsilon_y sin\theta cos\theta + \varepsilon_{xy}(cos^2\theta - sin^2\theta). \end{aligned} \tag{4}$$

These transformation equations involve square and products of sine and cosine functions and these can be replaced with double-angle results to yield the double-angle form of the transformation equations:

$$\begin{aligned} \varepsilon^{'}_x =& \frac{\varepsilon_x + \varepsilon_y}{2} + \frac{\varepsilon_x - \varepsilon_y}{2} cos2\theta + \varepsilon_{xy} sin2\theta \\ \varepsilon^{'}_y =& \frac{\varepsilon_x + \varepsilon_y}{2} - \frac{\varepsilon_x - \varepsilon_y}{2} cos2\theta - \varepsilon_{xy} sin2\theta \\ \varepsilon^{'}_{xy} =& \frac{\varepsilon_y - \varepsilon_x}{2} sin2\theta + \varepsilon_{xy} cos2\theta \end{aligned} \tag{5}$$

Good visualization of the transformation equations in the double-angle form considering geometrical correlations with Mohr's Circle can be found in ref. [8].

2.2 Extended strain gage rosette

The numerical simulation of the strain gate rosette is in contrast to the real electric device not limited to measure only strains. In a similar way as it was shown in section 2.1 it is now possible to get besides the projected principle strains the projected principle stresses in directions of each modeled gage as well. The corresponding stress transformation equations directly in double angle form are:

$$\begin{aligned} \sigma_x^{'} &= \frac{\sigma_x + \sigma_y}{2} + \frac{\sigma_x - \sigma_y}{2} cos2\theta + \tau_{xy} sin2\theta \\ \sigma_y^{'} &= \frac{\sigma_x + \sigma_y}{2} - \frac{\sigma_x - \sigma_y}{2} cos2\theta - \tau_{xy} sin2\theta \\ \tau_{xy}^{'} &= \frac{\sigma_y - \sigma_x}{2} sin2\theta + \tau_{xy} cos2\theta \end{aligned} \tag{6}$$

Knowing the rotation angle θ, this transformation equations can be applied to every relative to the coordinate system x_1, y_1 rotated system x_{2-6}, y_{2-6} (see Fig. 2) and define therefore the principal stresses in each of them.

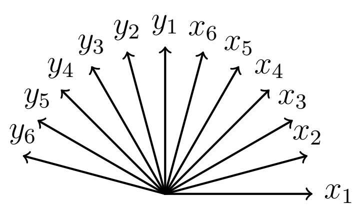

Figure 2: Extended strain gage

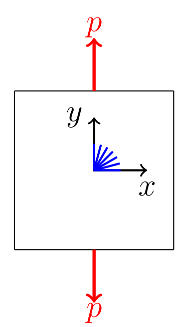

Figure 3: Gage arrangement

Consequently the computation of the projected principal strains and principal stresses in different coordinate systems arranged in the directions of each gage leads to the possibility to obtain an elastic moduli in every gage direction. For this purpose we consider a loading case according to Fig. 3 and relate the obtained results for the projected principal stresses with the results of the projected principal strains of every single gage through the generalized Hooke's Law. With ν defined as the Poisson's ratio and the assumptions $\sigma_z = 0, \tau_{xz} = 0$ and $\tau_{yz} = 0$ for plane stress follows:

$$\begin{aligned} \varepsilon_x &= \frac{\sigma_x}{E} - \nu \frac{\sigma_y}{E} \\ \varepsilon_y &= \frac{\sigma_y}{E} - \nu \frac{\sigma_x}{E} \\ \varepsilon_z &= -\nu \frac{\sigma_x}{E} - \nu \frac{\sigma_y}{E} \end{aligned} \tag{7}$$

The gages, depicted in blue in Fig. 3 can be evaluated on stress and strain according to the coordinate systems shown in Fig. 2 so that the formulations in Eq.(7) can be solved for the elastic moduli in every gage direction $(1-n)$:

$$\begin{aligned}
E_1 &= \frac{\sigma_{x_1}}{\varepsilon_{x_1}} - \nu\frac{\sigma_{y_1}}{\varepsilon_{x_1}} \\
&.. \\
E_n &= \frac{\sigma_{x_n}}{\varepsilon_{x_n}} - \nu\frac{\sigma_{y_n}}{\varepsilon_{x_n}}
\end{aligned} \tag{8}$$

2.3 Homogenization

2.3.1 Homogenized Poisson's ratio

The strain compatibility equations prescribe the necessary and sufficient conditions for continuous, single-valued displacements in single connected regions [9]. This continuous displacements in a deformed configuration of a series of finite elements that represent the composite material, can be measured through the in section 2.1 presented technique. Furthermore it can be shown (compare Fig. 4), that as long as the measured displacement fields are far away from the loading points (Saint-Venant's Principle), the measured values are independent of the size of the representing material section (RMS). To get the averaged elastic strains $\langle\varepsilon_{trans}\rangle$ and $\langle\varepsilon_{axial}\rangle$, the rosette is applied in a way that the gages labeled A,B and C are oriented at 45° apart as shown in Fig. 1-(a). Furthermore the rosette gage A is oriented to the principal averaged strains at the *angle* θ. The strain transformations shown in Eq. (5) can be used now to yield following relations:

$$\begin{aligned}
\varepsilon_A &= \frac{\langle\varepsilon_{trans}\rangle + \langle\varepsilon_{axial}\rangle}{2} + \frac{\langle\varepsilon_{trans}\rangle - \langle\varepsilon_{axial}\rangle}{2} cos2\theta \\
\varepsilon_B &= \frac{\langle\varepsilon_{trans}\rangle + \langle\varepsilon_{axial}\rangle}{2} + \frac{\langle\varepsilon_{trans}\rangle - \langle\varepsilon_{axial}\rangle}{2} cos2(\theta + 45^\circ) \\
\varepsilon_C &= \frac{\langle\varepsilon_{trans}\rangle + \langle\varepsilon_{axial}\rangle}{2} + \frac{\langle\varepsilon_{trans}\rangle - \langle\varepsilon_{axial}\rangle}{2} cos2(\theta + 90^\circ)
\end{aligned} \tag{9}$$

These three simultaneous equations can be inverted and solved for $\langle\varepsilon_{trans}\rangle$ and $\langle\varepsilon_{axial}\rangle$:

$$\langle\varepsilon_{trans,axial}\rangle = \pm\frac{1}{\sqrt{2}}\sqrt{(\varepsilon_A - \varepsilon_B)^2 + (\varepsilon_B - \varepsilon_C)^2} \tag{10}$$

Consequently the homogenized elastic constant Poisson's ratio can be obtained through the following relation:

$$\nu^* = -\frac{\langle\varepsilon_{trans}\rangle}{\langle\varepsilon_{axial}\rangle} \tag{11}$$

2.3.2 Homogenized Young's modulus

In Fig.8 there can be observed a periodic distribution of the stress fields. It is well known that isotropic material behave according to the Young's modulus in every direction the same. Section 3 demonstrates that there exist a coherence between the periodic stress field and the Young's modulus in the gage directions. In addition, it can be shown that the number of necessary gages converges to a certain value where no further approximation to the theoretical homogenized elastic modulus occurs. The necessary relations to obtain the homogenized Young's modulus build up the in Eq.(2.2)elaborated technique. Hereto the principal stresses in the gage directions of Eq.(6) are averaged over n sampling points located on each gage line:

$$\begin{aligned} \langle\sigma_{gage_i}\rangle_x &= \frac{1}{n}\sum_{k=0}^{n}\sigma_k, \\ \langle\sigma_{gage_i}\rangle_y &= \frac{1}{n}\sum_{k=0}^{n}\sigma_k \end{aligned} \tag{12}$$

To compute the average Young's modulus in the directions of the gages Eqs.(9), (10) and (12) can be inserted in Eq.(7):

$$\langle E_{gage_i}\rangle = \frac{1}{\varepsilon_{gage_i}}(\langle\sigma_{gage_i}\rangle_x - \nu^*\langle\sigma_{gage_i}\rangle_y) \tag{13}$$

Finally, the homogenized Young's modulus arise out of averaging over p gages of the in Eq.(13) computed values:

$$E^* = \frac{1}{p}\sum_{i=1}^{p}\langle E_{gage_i}\rangle \tag{14}$$

3 FEM MODELLING

In this section, the application of the homogenization method presented in Section 2 is performed on the example of a carbon/epoxy composite structure. The obtained results are compared with the results obtained through a Finite Element Multscale Direct Homogenization method presented by Borovkov [10]. The properties of the composite material are summarized in Table 1.

Table 1: Elastic properties and size definitions of the composite components

Composite Component	E $[MPa]$	ν	Periodic length $[m]$	Volume fraction
Epoxy matrix	3500	0,38	$2 \cdot 10^{-6}$ side length	0,8
Carbon fiber	34500	0,2	10^{-6} diameter	0,2

Beside the nearly conformity of the homogenized Young's modulus and Poisson's ratio it can be shown, that the presented method

- is independent of the size of the RMS,
- is independent of the length of the gages and

- converges to a homogenized Young's modulus for a sufficient quantity of gages.

Figure 4 shows in addition to the good match of the homogenized Poisson's ratio, the independence of the RMS size. The size of the gages is hereby controlled in a way that the ratio of the side length of the RMS to the gage length maintains a constant value of of $5:1$. This value arises from Fig. 5 where the gage length of 15 mm shows best match with the theory value of $0,34$ [10] on a RMS of size 76×76 μm.

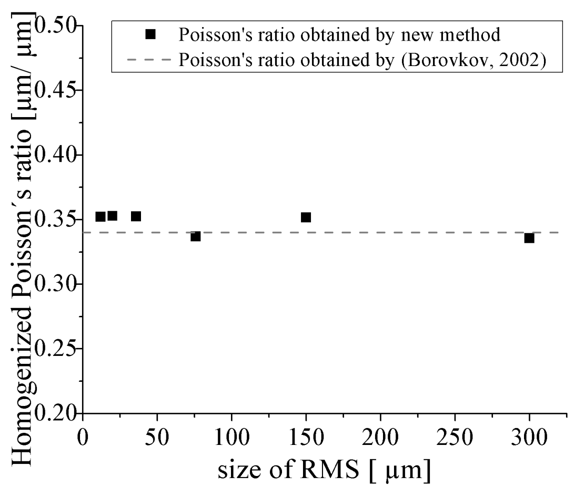

Figure 4: Size of RMS vs. Poisson's ratio

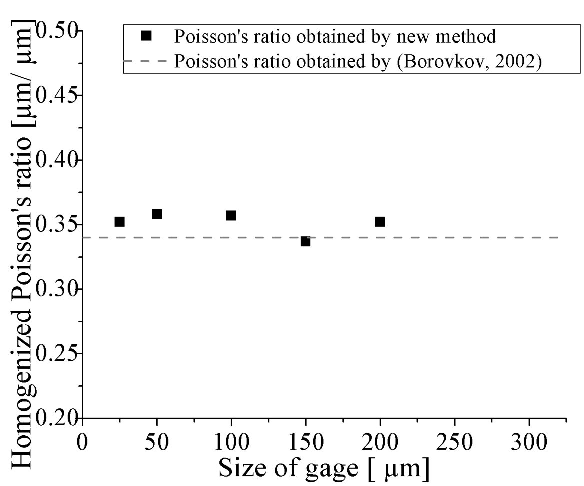

Figure 5: Size of gages vs. Poisson's ratio

Following pictures show the gate application on the composite structure and the resulting von-Mises stress according to the loading case shown in Fig. 3. Notably is the centered position of the gage and the periodic stress distribution.

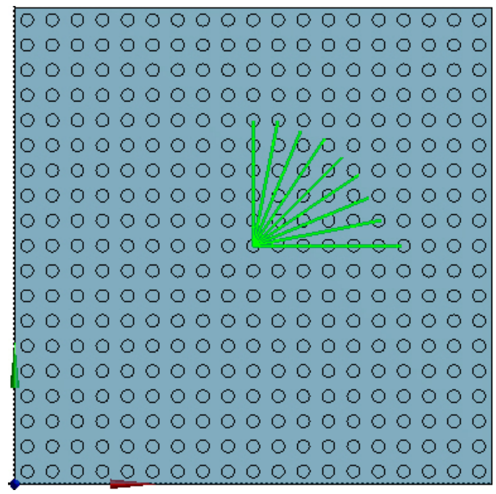

Figure 6: Gate orientation on RMS

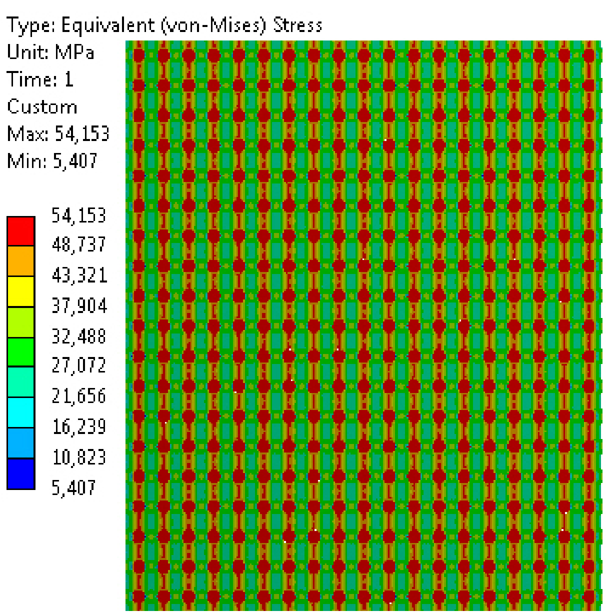

Figure 7: Von Mises stress

The new homogenization method is based on the computation of average stress values in different gage directions. The number of gage directions at least to be considered evokes from the convergence study presented in Fig.8. In case of the analyzed composite (Tab. 1) there are only seven directions needed to obtain the appropriate homogenized Young's modulus of 5270 MPA [10].

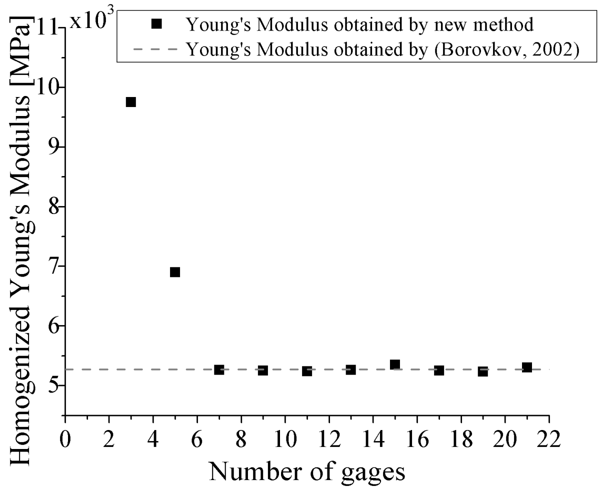

Figure 8: Convergence study for Youngs's Modulus over gage number

Following table summarizes finally the specifications made and results obtained by the new homogenization method:

Table 2: Results and specifications

loading case	RMS size $[m]$	Gage number	Gage size $[m]$	E^* $[MPa]$	ν^*
axial tension	$75 \cdot 10^{-6}$ side length	9	$10 \cdot 10^{-6}$	5122	0,377

4 CONCLUSIONS

This work described a new homogenization method that is capable of computing the homogenized elastic properties of a composite structure with high percentage of fibers. A very good match of the homogenization results (2.8% error for Young's modulus and 0.88% error for Poisson's ratio) with the results obtained by a Finite Element Multiscale Direct Homogenization method could be achieved. The low effort in modeling (only one loading case has to be considered) and the little computation time due to the small size of the RMS makes the presented method very effective. Furthermore it could be shown that there is no need of stochastic investigation for the RMS size nor the size of the gages.

Acknowledgement

L.P.P. acknowledges the financial support from the Chilean Agency CONICYT (FONDECYT project 1140583). C.A.R. acknowledges the financial support from the Chilean Agency CONICYT (FONDECYT project 1130417).

REFERENCES

[1] Sander, M., 2013, "Mathematische Homogenisierung in der Kontinuumsmechanik", Dissertation, Technische Universität Darmstadt.

[2] Eshelby, 1957, "The determination of the elastic field of an ellipsoidal inclusion, and related problems", Proceedings of the Royal Society of London. Series A, Mathematical and Physical Sciences.

[3] Li, 2007, "The Eshelby Tensors in a Finite Spherical Domain - Part 2: Applications to Homogenization",Journal of Applied Mechanics, Volume 74, 784-797.

[4] Gitman I.M., 2005, "Quantification of stochastically stable representative volumes for random heterogeneous materials", Arch Appl. Mech. 75: 79-92.

[5] Kanit T., 2003, "Determination of the size of the representative volume element for random composites: statistical and numerical approach", International Journal of Solids and Structures 40.

[6] Sharp,Jr. W.N. 2008, "Handbook of Experimental Solid Mechanics", Springer Handbooks, pp. 317-325.

[7] Sadd, M.H., 2011,"Elasticity. Theory, Applications, and Numerics", Academic Press, 2nd Ed., pp. 34-38.

[8] Popov, E.P., 2000, "Mecánicos de Sólidos", Pearson Educación, México, 2nd Ed., pp.481-490.

[9] Sadd, M.H., 2011,"Elasticity. Theory, Applications, and Numerics", Academic Press, 2nd Ed., pp. 41-46.

[10] Borovkov, A.I., 2002,"Finite Element Multiscale Homogenization and Sequential Heterogenization of Composite Structures", Int. ANSYS Conf. 132.